Edge-aware Regional Message Passing Controller for Image Forgery Localization

Dong Li, Jiaying Zhu, Menglu Wang, Jiawei Liu, Xueyang Fu, Zheng-Jun Zha
{dongli6, zhujy53, vault}@mail.ustc.edu.cn, {jwliu6, xyfu, zhazj}@ustc.edu.cn

University of Science and Technology of China, China
Poster: TUE-PM-393

Quick Preview

- We propose a novel method to avoid feature coupling of the forged regions and authentic regions for image forgery localization: **Edge-Aware Region Message Passing Controller** (ERMPC).
- Graph convolutions can control the message passing between two regions by tuning the adjacency matrix.
- Taking edge information as the main task and using it as a basis to explicitly model the inconsistency.

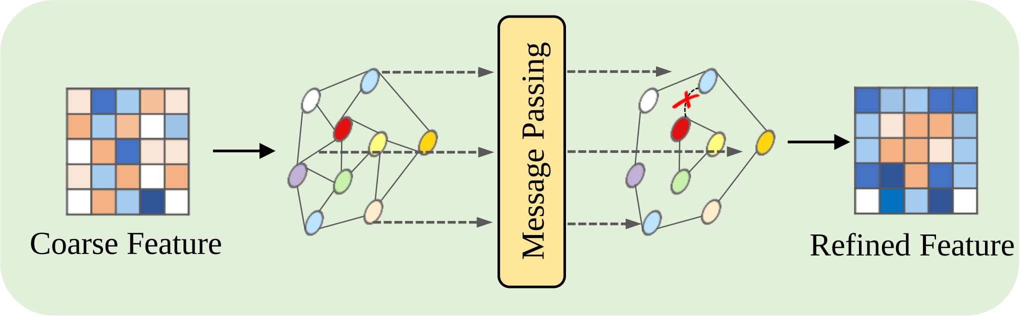

The graph controls the message passing

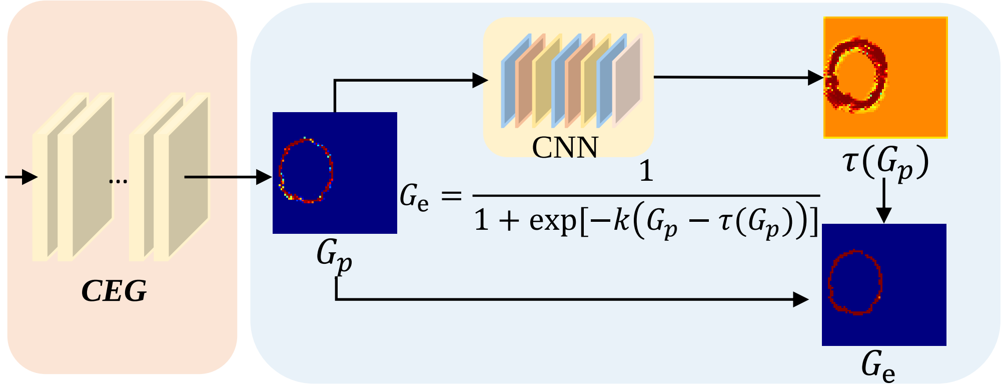

Edge reconstruction

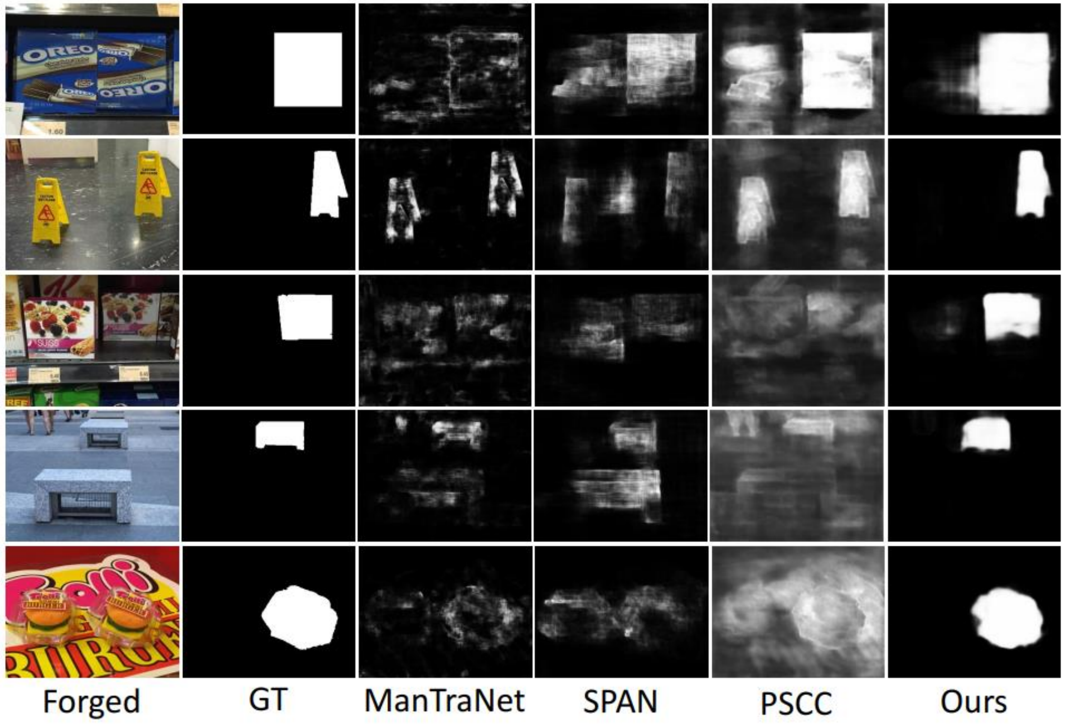

Background

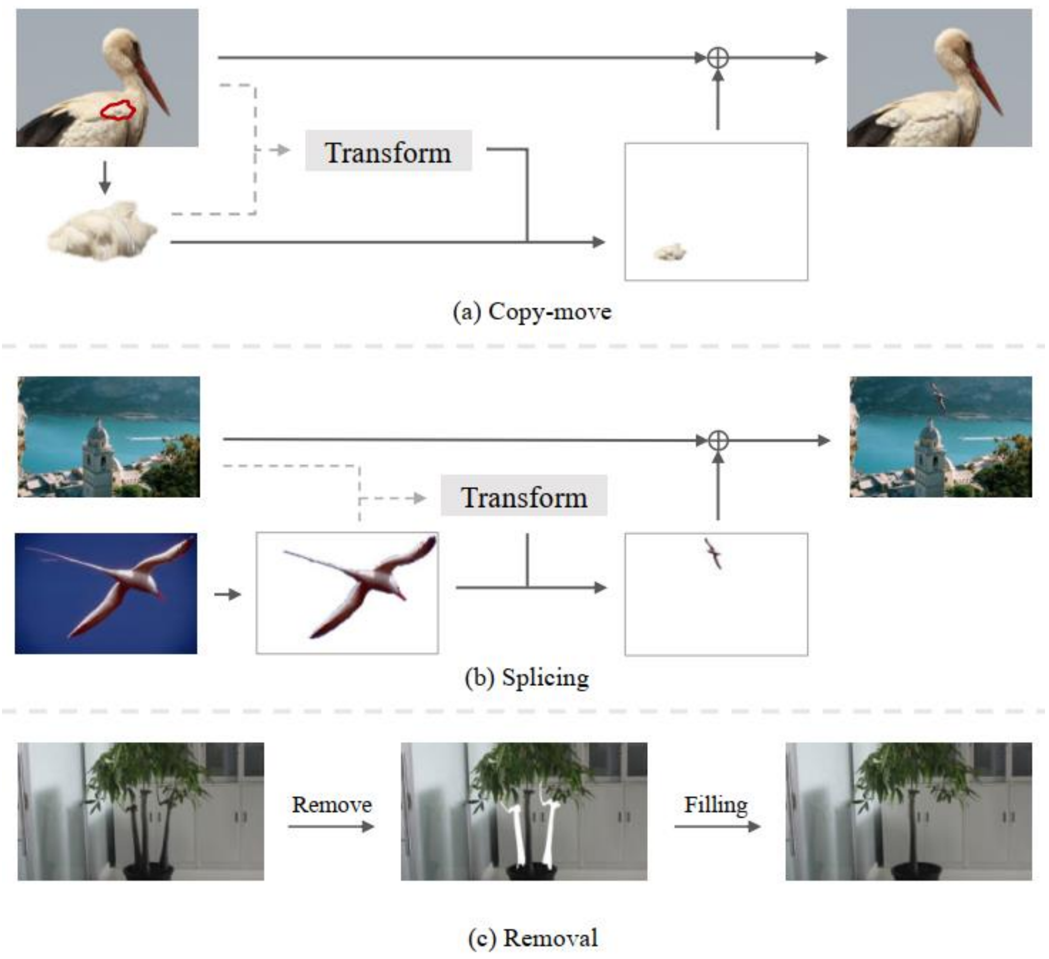

Forged images pose risks to society.

Wang, Junke, et al. "Fighting Malicious Media Data: A Survey on Tampering Detection and Deepfake Detection." arXiv:2212.05667 (2022).

Introduction

- Previous methods usually **suffer from severe feature coupling** between the forged and authentic regions.
- We **control the message passing** between the forged and authentic regions to locate the tampered regions for elaborately forged images accurately.

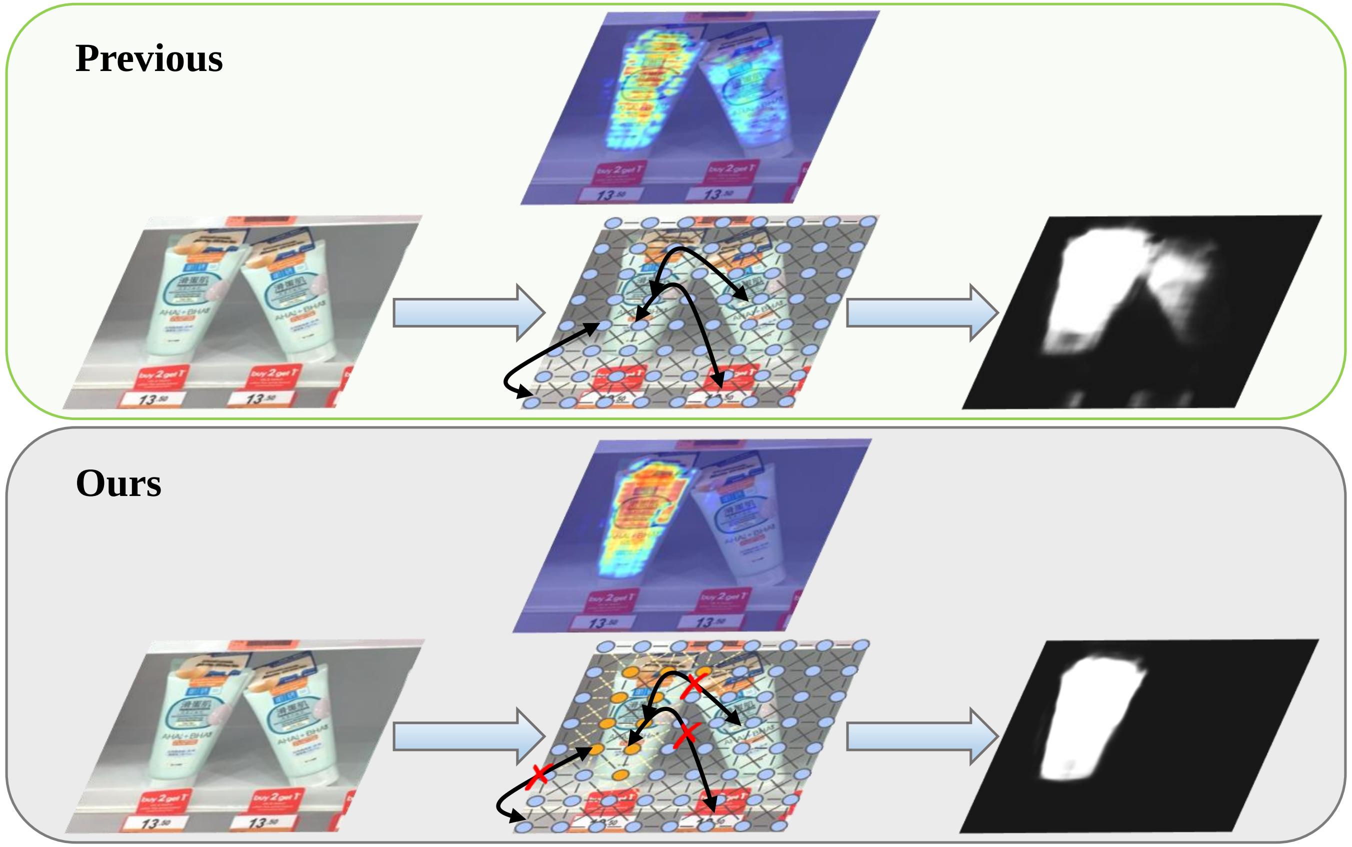

Methods

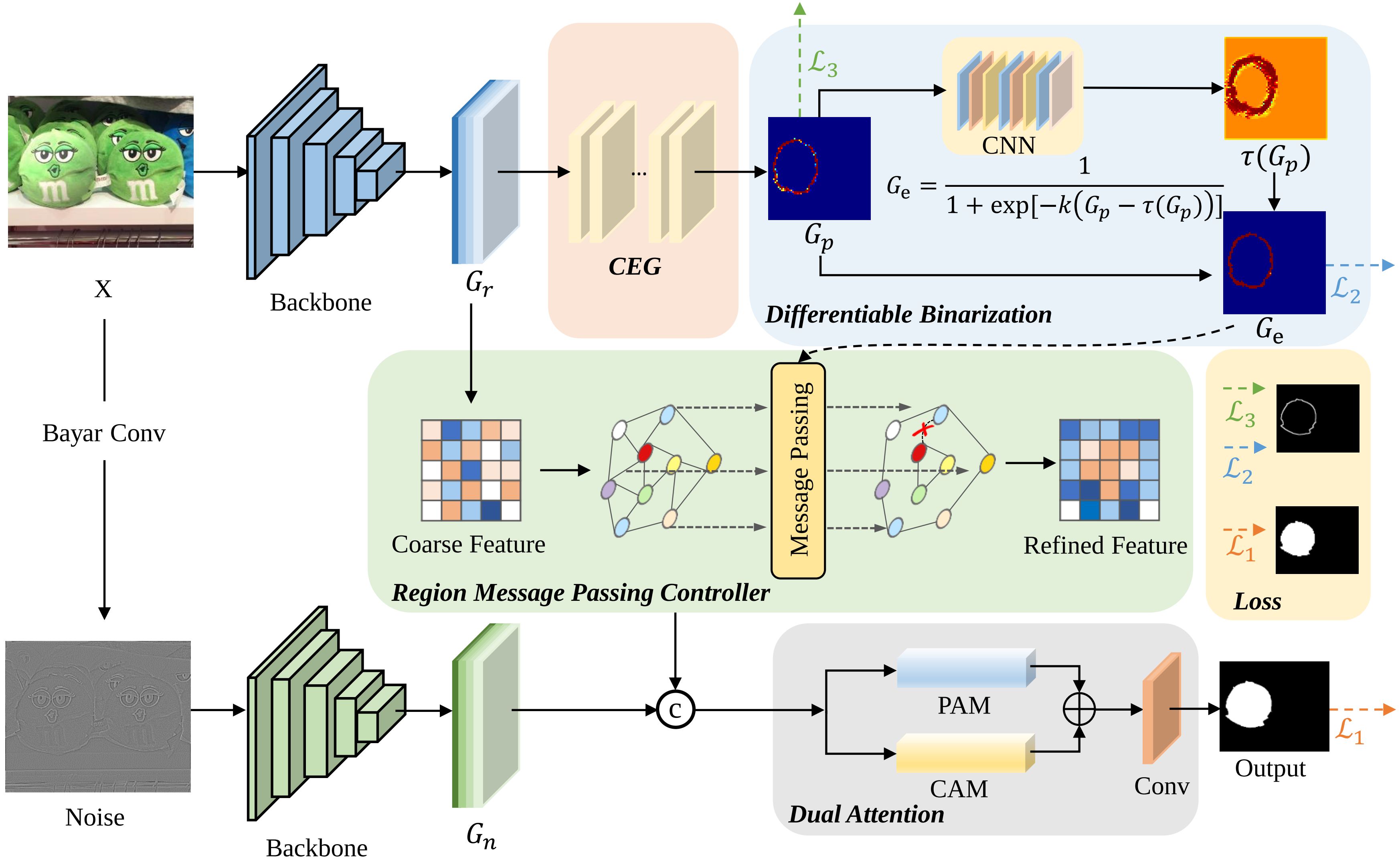

The overview of our proposed Edge-Aware Region Messaging Controller (ERMPC).

Methods

$$XN(P_i, P_j) = \begin{cases} 0 & \textit{Inside and outside the edges} \\ 1 & \textit{On the same side of edges} \end{cases}$$

For each of the N ($N = H_e \times W_e$) nodes features, we calculate its XN, thus generating the **matrix** $A_e \in \mathbb{R}^{N\times N}$.

$$\psi = Wx \qquad \psi' = W'x$$

$$\alpha_{i,j} = \psi(x_i)^T \psi'(x_j)$$

$$A_{r_{i,j}} = \frac{\exp(\alpha_{i,j})}{\sum_{j=1}^{N} \exp(\alpha_{i,j})}$$

Following Graph Attention Network(GAT) , we calculate the adjacency **matrix** $A_r \in \mathbb{R}^{N\times N}$ of the feature map.

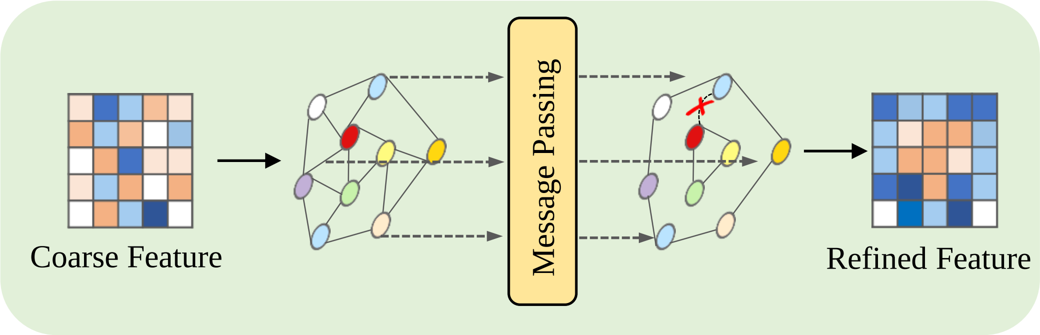

Region Message Passing Controller (RMPC)

$$A'_r = A_r \odot A_e$$

$$Z_r = ReLU(A'_r G'_r W_z)$$

We take the Hadamard product of two matrices to obtain the dynamic adjacency **matrix** $A'_r \in \mathbb{R}^{N\times N}$.

Methods

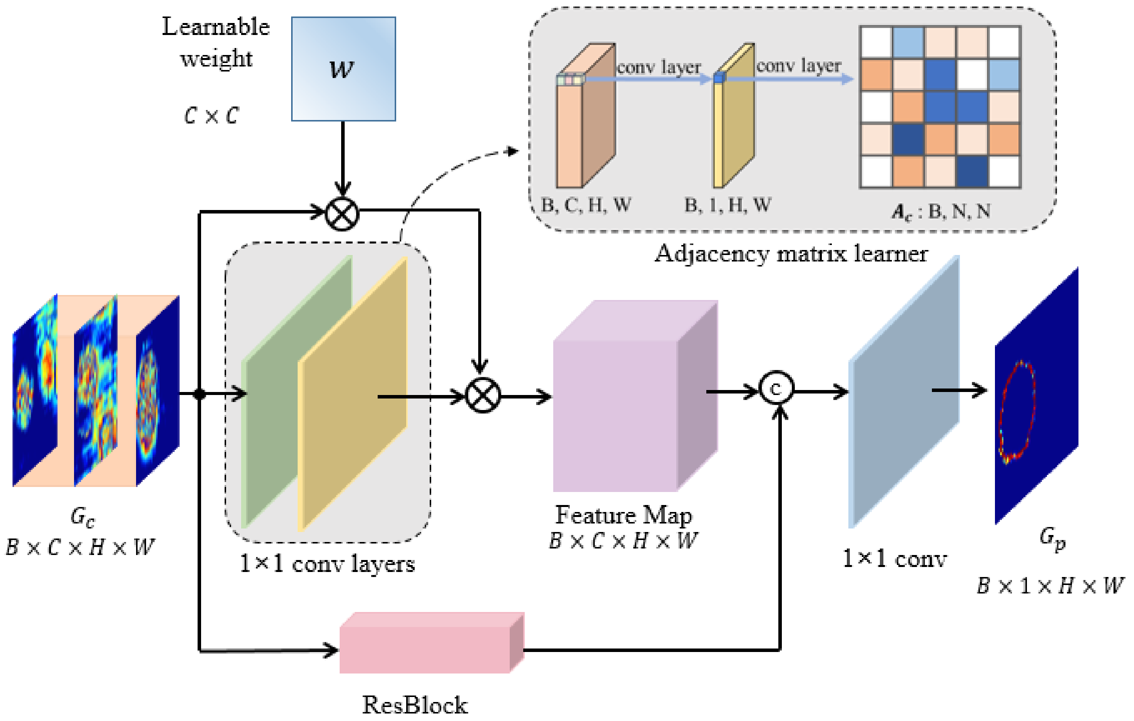

Context-enhanced graph (CEG).

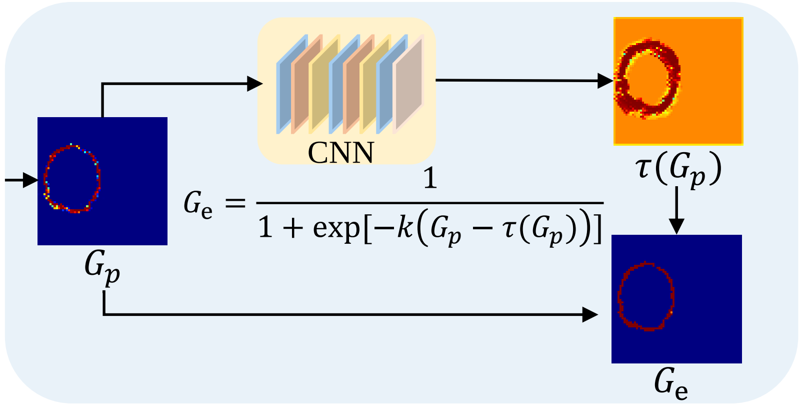

Threshold-adaptive differentiable binarization module (TDB).

Experiments

Quantitative results

Method	Data	Columbia	Coverage	CASIA	NIST16	IMD20
ManTraNet	64K	82.4	81.9	81.7	79.5	74.8
SPAN	96k	93.6	92.2	79.7	84.0	75.0
PSCCNet	100k	**98.2**	84.7	82.9	85.5	80.6
ObjectFormer	62K	95.5	92.8	84.3	87.2	82.1
Ours	60K	96.8	**94.4**	**87.6**	**89.5**	**85.6**

Table 1. Comparisons of manipulation localization AUC (%) scores of different pre-trained models.

Methods	Coverage		CASIA		NIST16	
	AUC	F1	AUC	F1	AUC	F1
J-LSTM	61.4	-	-	-	76.4	-
H-LSTM	71.2	-	-	-	79.4	-
RGB-N	81.7	43.7	79.5	40.8	93.7	72.2
SPAN	93.7	55.8	83.8	38.2	96.1	58.2
PSCCNet	94.1	72.3	87.5	55.4	99.1	74.2
ObjectFormer	95.7	75.8	88.2	57.9	99.6	82.4
Ours	**98.4**	**77.3**	**90.4**	**58.6**	**99.7**	**83.6**

Table 2. Comparison of manipulation localization results using fine-tuned models.

Experiments

Robustness evaluation

Distortion	SPAN	ObjectFormer	Ours
no distortion	83.95	87.18	**89.49**
Resize($0.78\times$)	83.24	87.17	**89.33** **0.16↓**
Resize($0.25\times$)	80.32	86.33	**87.72** **1.77↓**
Blur($k=3$)	83.10	85.97	**89.22** **0.27↓**
Blur($k=15$)	79.15	80.26	**87.13** **2.36↓**
Noise($\sigma=3$)	75.17	79.58	**88.25** **1.24↓**
Noise($\sigma=15$)	67.28	78.15	**83.40** **6.09↓**
Compress($q=100$)	83.59	86.37	**89.42** **0.07↓**
Compress($q=50$)	80.68	86.24	**88.82** **0.67↓**

Table 3. Localization performance on NIST16 dataset under various distortions. AUC scores are reported (in %), (Blur: GaussianBlur, Noise: GaussianNoise, Compress: JPEGCompress.)

Experiments

Qualitative results

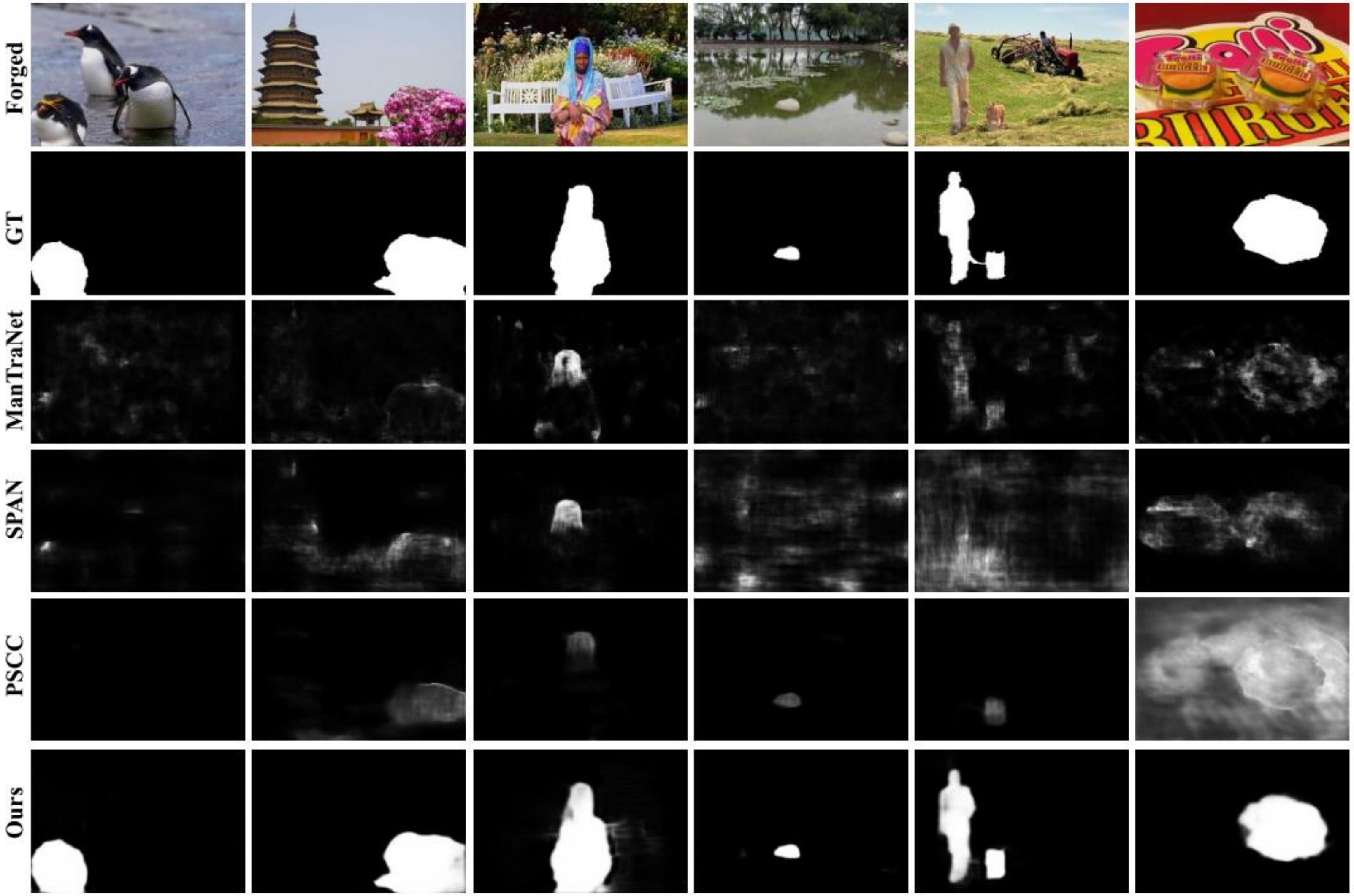

Figure 4. Visualization of the predicted manipulation mask by different methods. From top to bottom, we show forged images, GT masks, predictions of ManTraNet, SPAN, PSCC-Net, and ours.

Ablation

Variants	CASIA		NIST16	
	AUC	F1	AUC	F1
Baseline	71.6	38.3	77.1	52.6
w/o RMPC	76.9	45.6	86.4	60.7
w/o CEG	85.1	51.5	93.4	75.3
w/o TDB	88.6	57.3	98.2	81.9
Ours	**90.4**	**58.6**	**99.7**	**83.6**

Table 4. Ablation results on CASIA and NIST16 dataset using different variants of ERMPC. AUC and F1 scores (%) are reported.

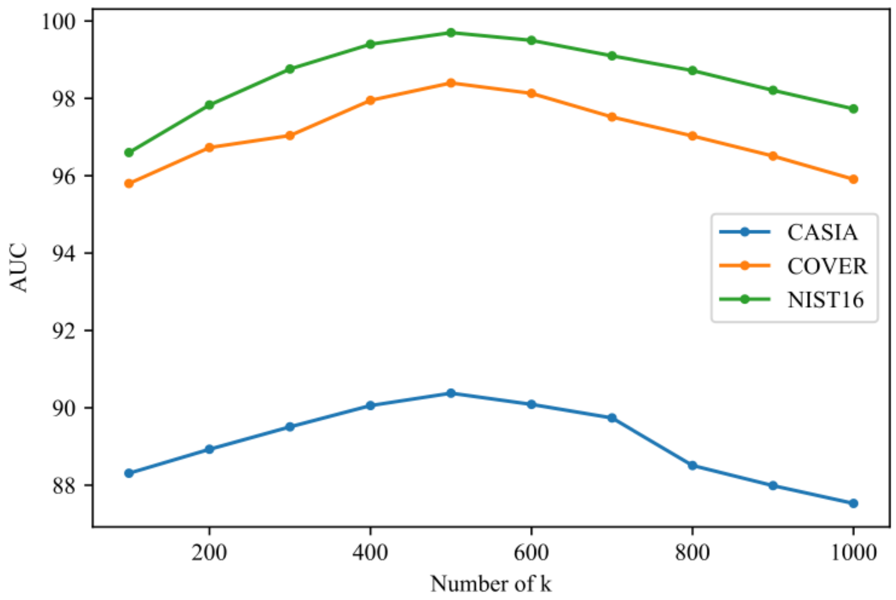

Figure 5. The effect of parameter k in TDB

Experiments

Visualizations

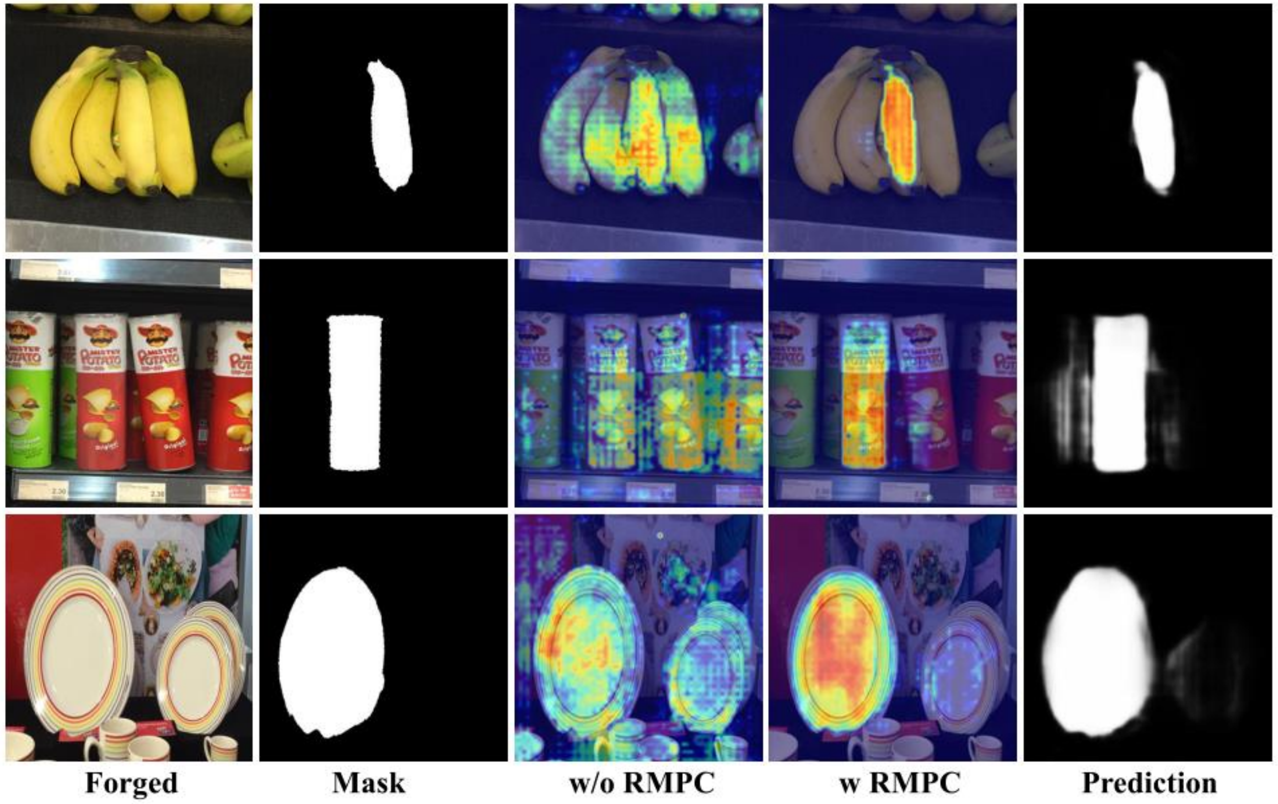

Figure 6. Visualization of message passing controller. From left to right, we display the forged images, masks, GradCAM [42] of the feature map without (w/o) and with (w) RMPC, and predictions.

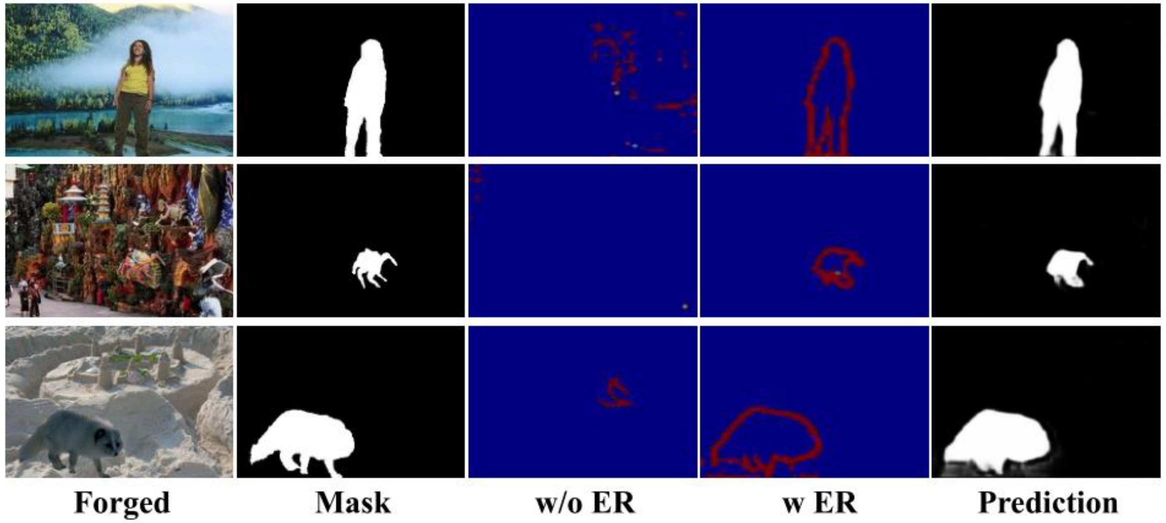

Figure 7. Visualization of edge reconstruction. From left to right, we display the forged images, masks, the features without (w/o) and with (w) the edge reconstruction module, and prediction.

Conclusion

- We propose ERMPC, a novel **two-step coarse-to-fine framework** for image forgery localization, using edge information **to explicitly model the inconsistency** between forged and authentic regions. It provides a new research strategy to **solve the misjudgment problem** in the field of image forgery localization.

- We propose an **edge-aware dynamic graph**, also known as RMPC, to control the message passing between two regions (forged and authentic) in the feature map.

- We develop an **edge reconstruction** module containing a context-enhanced graph and a threshold-adaptive differentiable binarization module to obtain the desired edge information.

- Extensive experimental results on several benchmarks demonstrate the effectiveness of the proposed algorithm.